

# Compact Physical Models for Gate Charge and Gate Capacitances of AlGa<sub>N</sub>/Ga<sub>N</sub> HEMTs

F.M. Yigletu and B. Iñiguez

Dept. of Electrical Electronics and Automation Engineering  
Universitat Rovira i Virgili  
Tarragona, Spain  
e-mail: [fetenemulugeta.yigletu@urv.cat](mailto:fetenemulugeta.yigletu@urv.cat)

S. Khandelwal and T.A. Fjeldly

Dept. of Electronics and Telecommunication  
Norwegian University of Science and Technology, NTNU  
Trondheim, Norway  
e-mail: [torfj@unik.no](mailto:torfj@unik.no) or [sourabh.khandelwal@ntnu.no](mailto:sourabh.khandelwal@ntnu.no)

**Abstract**— This work presents a physical analytical model for the total gate charge and C-V characteristics of AlGa<sub>N</sub>/Ga<sub>N</sub> HEMT devices. A continuous analytical model of the gate-charge is developed first, based on an assumption of considering only the first energy level in the triangular quantum well approximation at the AlGa<sub>N</sub>/Ga<sub>N</sub> interface where most of charge carriers reside. The gate-source and the gate-drain capacitances are then obtained through differentiation of the gate charge at the corresponding terminal voltages. Excellent agreements between the modeled and measured C-V characteristics of a device were obtained.

**Keywords**— HEMTs, Power Amplifiers, power transistors, Semiconductor Device Modeling, Simulation

## I. INTRODUCTION

After a series of extensive research works in the past years demonstrated the suitability of AlGa<sub>N</sub>/Ga<sub>N</sub> HEMTs for high power and high frequency applications [1-3], currently it is becoming quite common to find these devices in commercial products such as RF power amplifiers [4]. This obviously has increased the need for models of these devices for circuit simulation. Since the basic principle of operation of these devices is based on the 2DEG that is formed at the heterostructure interface, accurate modeling of the charge and capacitances at the interface is critical. Compact physics-based models are desirable for this purpose as they provide higher accuracy while keeping a minimum set of parameters. Since there are different Fermi potentials and energy levels that should be considered while developing such physical models, coming up with simpler models keeping a higher accuracy is a challenging task.

In this work we present a physical analytical model for the gate-source and gate-drain capacitances. A continuous total gate charge model is developed first from which the capacitances are derived through differentiation with respect to the terminal voltages. The gate charge model is developed base on a simple unified charge control model that is obtained using an assumption of considering only a single energy level in the triangular quantum well approximation at the AlGa<sub>N</sub>-Ga<sub>N</sub> heterostructure interface. A drain current model developed based on this was presented in an earlier work [5]. The development and derivation of the total gate charge and capacitance models is presented in section II. Then in section III, simulation results and

Table I  
List of Symbols

<i>symbol</i>	<i>Description</i>
$q$	The electron charge
$V_{th}$	Thermal Voltage
$\epsilon$	The dielectric permittivity of AlGa <sub>N</sub>
$d$	Thickness of AlGa <sub>N</sub> layer
$E_f$	Position of the Fermi level
$E_0$	Position of the first energy level in the triangular quantum well
$E_1$	Position of the second energy level in the triangular quantum well
$D$	Density of states
$\gamma_0, \gamma_1$	Parameters determined from experiment
$n_s$	Density of electron in the 2DEG
$C_g$	Gate Capacitance per unit area ( $\epsilon/d$ )

comparisons with measurement data are shown and discussed. Finally the conclusion is given in section IV.

## II. ANALYTICAL MODEL

The gate charge expression is developed using a simple charge control model as described in sub-section A. Once the complete charge expression is developed the gate-source and gate-drain capacitances are derived.

### A. Charge model

In heterostructures such as AlGa<sub>N</sub>/Ga<sub>N</sub> and AlGaAs/GaAs the charge density accumulated in the potential well at the interface can be calculated with the assumption of a quasi-constant electric field in the potential well (triangular well approximation) and two sub-bands as [6]

$$n_s = DV_{th} \left[ \ln \left( e^{(E_f - E_0)/V_{th}} + 1 \right) + \ln \left( e^{(E_f - E_1)/V_{th}} + 1 \right) \right]. \quad (1)$$

This work is supported by the European Commission Project, CoMoN, under the Grant Agreement 218255.

These sub-bands are given as [7]

$$E_0 = \gamma_0 n_s^{2/3} \text{ and } E_1 = \gamma_1 n_s^{2/3} \quad (2)$$

where  $\gamma_0$  and  $\gamma_1$  are constants estimated from Shubnikov De Hass or cyclotron resonance experiments [6]. When the gate depletion and channel depletion overlap to give a fully depleted barrier layer the carrier density is given by [8]

$$n_s = \frac{\epsilon}{qd} (V_{g0} - E_f) \quad (3)$$

where  $V_{g0} = V_g - V_{off}$ , where  $V_{off}$  is the cut-off voltage.

In the triangular quantum well created at the interface of AlGa<sub>x</sub>N/GaN the second energy level is much higher than the first one and is well above the Fermi level for the whole operating range of the gate voltage [9]. Thus, in the approach used here, the contribution of only the first energy level is considered. Therefore, (1) can be written as

$$n_s = DV_{th} \ln \left( \exp \left( \frac{E_f - E_0}{V_{th}} \right) + 1 \right). \quad (4)$$

The expressions of  $E_0$  and  $E_f$  from (2) and (3) respectively can be used in (4) to establish a simple charge control model given as

$$V_{g0} = \frac{qdn_s}{\epsilon} + \gamma_0 n_s^{2/3} + V_{th} \ln \left[ \exp \left( \frac{n_s}{DV_{th}} \right) - 1 \right]. \quad (5)$$

The exponential term in (5) can be expanded into a Taylor series and the first few terms can be used. In fact, the first term gives a good approximation. In addition, (5) can be extended to any channel point by considering  $V$  as the local quasi-Fermi potential. Therefore, we have

$$V_{g0} - V = \frac{qdn_s}{\epsilon} + \gamma_0 n_s^{2/3} + V_{th} \ln \left( \frac{n_s}{DV_{th}} \right). \quad (6)$$

The simple charge control model in (6) is valid in all operation regimes and gives an important relation between the applied voltage and the charge carrier concentration which can be used to derive the gate charge model and thereby the gate capacitances. The gate charge can be obtained by integrating the charge density along the channel over the gate area

$$Q_G = W \int_0^L qn_s(x) dx \quad (7)$$

where  $L$  is the channel length and  $W$  is the channel width of the device. From a similar expression of the drain-source current,  $dx$  can be substituted which will change the integration variable from  $x$  to  $V$ . Therefore, we have

$$Q_G = \frac{W^2 q^2 \mu}{I_{ds}} \int_{V_s}^{V_d} n_s^2 dV \quad (8)$$

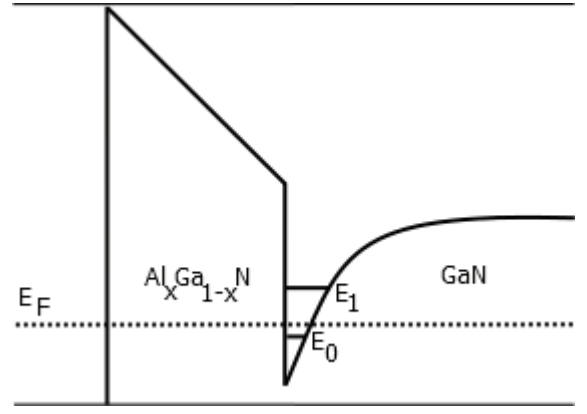


Fig. 1. Heterostructure interface and Energy band profile of an AlGa<sub>x</sub>N/GaN HEMT.

where  $\mu$  is the low field mobility and  $I_{ds}$  is the drain source current that is given as

$$I_{ds} = \frac{Wq\mu}{L} \int_{V_s}^{V_d} n_s dV. \quad (9)$$

Substituting (9) in (8) gives the total gate charge as

$$Q_G = WLq \frac{\int_{V_s}^{V_d} n_s^2 dV}{\int_{V_s}^{V_d} n_s dV}. \quad (10)$$

The derivative of the voltage w.r.t  $n_s$ , can be obtained from (6) and is given as

$$dV = - \left( \frac{qd}{\epsilon} + \frac{2}{3} \gamma_0 n_s^{-1/3} + V_{th} n_s^{-1} \right) dn_s. \quad (11)$$

The two integrals at the numerator and denominator in (10) can be represented as  $f(n_s)$  and  $g(n_s)$  respectively and integrating after changing the integration variable using the relations between  $dV$  and  $dn_s$ , (11), gives

$$f(n_s) = \frac{qd}{3\epsilon} (n_D^3 - n_S^3) + \frac{1}{4} \gamma_0 (n_D^{8/3} - n_S^{8/3}) + \frac{1}{2} V_{th} (n_D^2 - n_S^2) \quad (12)$$

$$g(n_s) = \frac{qd}{2\epsilon} (n_D^2 - n_S^2) + \frac{2}{5} \gamma_0 (n_D^{5/3} - n_S^{5/3}) + V_{th} (n_D - n_S) \quad (13)$$

where  $n_S$  and  $n_D$  are the charge carrier densities calculated at the source and drain respectively [5].

The gate charge then becomes

$$Q_G = WLq \frac{\frac{qd}{3\epsilon} (n_D^3 - n_S^3) + \frac{1}{4} \gamma_0 (n_D^{8/3} - n_S^{8/3}) + \frac{1}{2} V_{th} (n_D^2 - n_S^2)}{\frac{qd}{2\epsilon} (n_D^2 - n_S^2) + \frac{2}{5} \gamma_0 (n_D^{5/3} - n_S^{5/3}) + V_{th} (n_D - n_S)}. \quad (14)$$

$n_S$  and  $n_D$  can be obtained iteratively from (6). Instead, using sufficiently accurate explicit expressions would make the model computationally faster. We have used an approximate unified

explicit expression that covers all the operating regions from deep subthreshold to full active gate bias to obtain the charge carrier concentrations at the source and drain [9].

Note that  $g(n_s)$  is the integral part of the definition of the drain current given in (9), i.e.  $g(n_s) = -I_{ds}L / q\mu W$  and the drain current is given as [5]

$$I_{ds} = -\frac{q\mu W}{L} \left[ \frac{qd}{2\epsilon} (n_D^2 - n_S^2) + \frac{2}{5} \gamma_0 (n_D^{5/3} - n_S^{5/3}) + V_{th} (n_D - n_S) \right]. \quad (15)$$

### B. Gate-Source and Gate-Drain Capacitances

The gate-source and the gate-drain capacitances can now be calculated using the partial derivatives of the gate charge in terms of the corresponding source and drain terminal voltages. Therefore, the capacitances are obtained as

$$C_{Gx} = WLq \frac{\frac{\partial f(n_s)}{\partial V_x} g(n_s) - f(n_s) \frac{\partial g(n_s)}{\partial V_x}}{(g(n_s))^2} \quad (16)$$

where  $V_x = V_s$  and  $C_{Gx} = C_{GS}$  at the source terminal and

$V_x = V_d$  and  $C_{Gx} = C_{GD}$  at the drain terminal.

However,  $f(n_s)$  and  $g(n_s)$  can also be defined as

$$f(n_s) = f_{main}(n_D) - f_{main}(n_S) \quad (17)$$

$$g(n_s) = g_{main}(n_D) - g_{main}(n_S) \quad (18)$$

where

$$f_{main}(n_x) = \frac{qd}{3\epsilon} n_x^3 + \frac{1}{4} \gamma_0 n_x^{8/3} + \frac{1}{2} V_{th} n_x^2 \quad (19)$$

$$g_{main}(n_x) = \frac{qd}{2\epsilon} n_x^2 + \frac{2}{5} \gamma_0 n_x^{5/3} + \frac{1}{2} V_{th} n_x \quad (20)$$

where  $n_x = n_D$  at the drain terminal and  $n_x = n_S$  at the source terminal. From (19) and (20) the derivatives of  $f_{main}(n_x)$  and  $g_{main}(n_x)$  can be written as

$$\frac{df_{main}(n_x)}{dV_x} = \left( \frac{qd}{\epsilon} n_x^2 + \frac{2}{3} \gamma_0 n_x^{5/3} + V_{th} n_x \right) \frac{dn_x}{dV_x} \quad (21)$$

$$\frac{dg_{main}(n_x)}{dV_x} = \left( \frac{qd}{\epsilon} n_x + \frac{2}{3} \gamma_0 n_x^{2/3} + V_{th} \right) \frac{dn_x}{dV_x} \quad (22)$$

where  $dn_x/dV_x$  can be obtained from (11). We can see from (17) and (18) that the partial derivatives of  $f(n_s)$  and  $g(n_s)$  are equivalent to the derivatives of

$f_{main}(n_x)$  and  $g_{main}(n_x)$  at the respective terminals which are given by (21) and (22). Therefore, the gate-source and the gate-drain capacitances can now be expressed as

$$C_{Gx} = WLq \frac{\frac{df_{main}(n_s)}{dV_x} g(n_s) - f(n_s) \frac{dg_{main}(n_s)}{dV_x}}{(g(n_s))^2}. \quad (23)$$

### III. RESULTS AND DISCUSSION

Simulations of the C-V characteristics have been carried out and the results were compared with measurements of a device obtained from [10]. The device has gate length of 0.35 $\mu$ m. The gate-source capacitance is plotted against the gate voltage as shown in Fig.1.

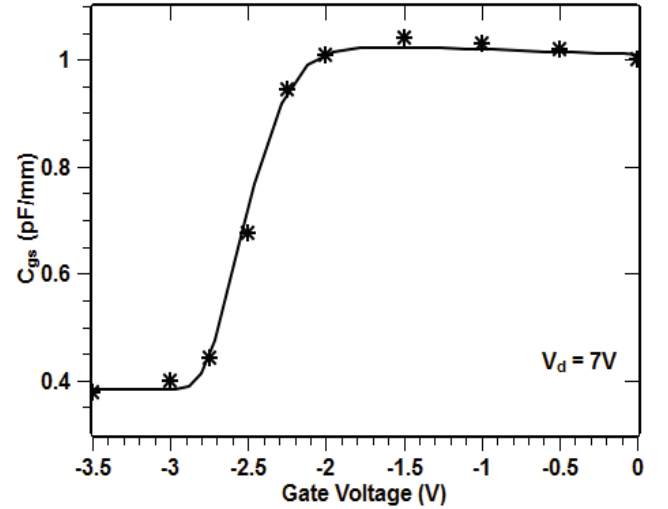


Fig. 1. Measured (symbols) and modeled (solid lines) gate-source capacitance  $C_{gs}$  of a device with a gate length of 0.35 $\mu$ m at a drain voltage of 7V, data from [10].

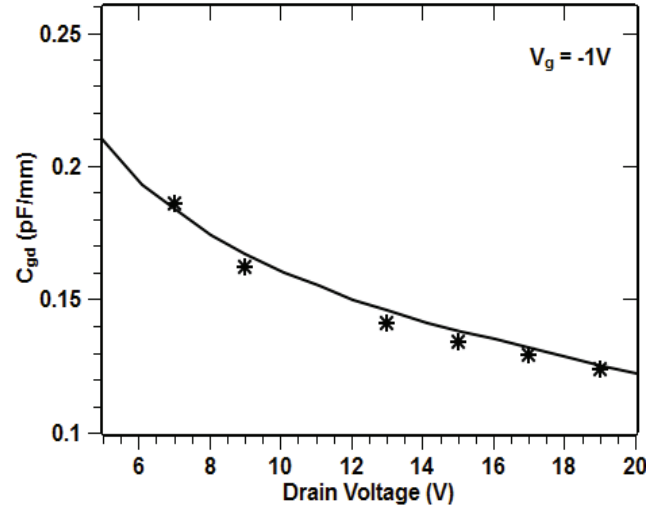


Fig. 2. Measured (symbols) and modeled (solid lines) gate-drain capacitance  $C_{gd}$  of a device with a gate length of 0.35 $\mu$ m at a gate voltage of -1V, data from [10].

Here we show the plot of  $C_{gs}$  at one specific drain voltage,

7V in this case, as the dependence of  $C_{gs}$  on the drain source voltage is very small. The simulated and measured  $C_{gs}$  showed a good agreement. Fig.2 shows the gate-drain capacitance plotted against the drain voltage. Again there is a good agreement between measurement and simulation.

In addition the output I-V characteristics are also shown in Fig.3 to further confirm the consistency of the capacitance model with the drain current model.

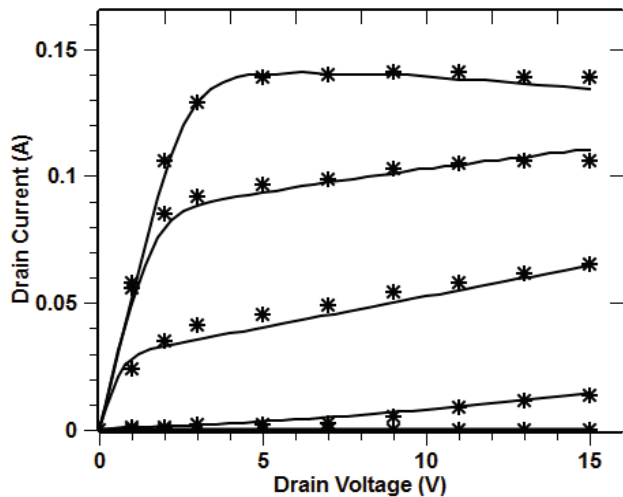


Fig.3. Measured (symbols) and modeled (solid lines) output characteristics of a device with a gate length of  $0.35\mu\text{m}$  when the gate voltage varies from  $-4\text{V}$  to  $0\text{V}$  with a step of  $1\text{V}$ , bottom to top, data from [10].

#### IV. CONCLUSION

Analytical physics-based models for the gate charge and the C-V characteristics of AlGaIn/GaN HEMT devices have been presented. A continuous analytical charge model is developed using a charge carrier concentration model where only the contribution of the first energy level of a triangular quantum well is considered. The assumption of considering only the first energy level in triangular quantum well allowed to establish a simple relationship between the applied voltage and the charge carrier concentration. This assumption is valid to the AlGaIn/GaN material composition where a considerable part of the 2DEG at the heterostructure interface is located at the first energy level and might not be applicable to triangular quantum well approximation of other heterostructures where the 2DEG is fairly distributed between the first and the second energy levels. The total charge is obtained by integrating the charge density along the channel and the gate-source and the gate-drain capacitances are then obtained by differentiating the total gate charge with respect to the source and drain terminal voltages respectively. The good agreement between measured and modeled C-V characteristics validates the model.

#### ACKNOWLEDGMENT

The authors would like to thank the European Commission project, CoMoN, under the Grant Agreement 218255.

#### REFERENCES

- [1] P. Kordos, A. Alam, J. Betko, P.P. Chow, M. Heuken, P. Javorka, M. Kocan, M. Marso, M. Morvic and J.M. Van Hove, "Material and device issues of GaN-based HEMTs," *8th IEEE International Symposium on High Performance Electron Devices for Microwave and Optoelectronic Applications*, pp. 61-66, Nov. 2002.
- [2] P. Parikh, Y. Wu, M. Moore, P. Chavarkar, Mishra, R. Neidhard, L. Kehias, T. Jenkins, "High linearity, robust, AlGaIn-GaN HEMTs for LNA and receiver ICs," *Proceedings of IEEE Lester Eastman Conference on High Performance Devices*, pp. 415-421, Aug. 2002.
- [3] W.L. Pribble, J.W. Palmour, S.T. Sheppard, T.J. Smith, J.J. Sumakeris, A.W. Saxler, J.W. Milligan, "Applications of SiC MESFETs and GaN HEMTs in power amplifier design," *IEEE MTT-S International Microwave symposium digest*, vol. 3, pp. 1819-1822, June 2002.
- [4] Danqiong Hou, Griff L. Bilbro, and Robert J. Trew, "Analytical Model for Conduction Current in AlGaIn/GaN HEMTs/HEMTs," *Active Passive Electron. Compon.*, vol. 2012, pp. 806253-1 - 806253-11, Jan. 2012
- [5] F.M Yigletu, B. Iñiguez, S. Khandelwal and T.A. Fjeldly, *proceedings of 2013 IEEE Radio and Wireless Week*, pp. 103-105, January 2013, Austin TX, USA.
- [6] D. Delegebeaudeuf and N.T Linh, "Metal-(n)AlGaAs-GaAs two dimensional electron gas FET," *IEEE electron Device Lett.*, vol. ED-29, no. 6, pp. 955-960, June 1982.
- [7] S. Kola, J.M. Golio, and G.N. Maracas, "An analytical expression for Fermi level versus carrier concentration for HEMT modeling," *IEEE Electron Device Lett.*, vol.9, no.3, pp. 136-138, March 1988.
- [8] K. Lee, M. Shur, T. J. Drummond, H. Morkoc, "Current-voltage and capacitance-voltage characteristics of modulation doped field-effect transistors," *IEEE Trans. Electron Devices*, vol. ED-30, no. 3, pp. 207-212, March 1983.
- [9] S. Khandelwal, N. Goyal, T.A. Fjeldly, "A physics based analytical model for 2DEG charge density in AlGaIn/GaN HEMT devices," *IEEE Trans. Elect. Devices*, vol. 58, no. 10, pp. 3622-3625, Oct. 2011.
- [10] J.W.Lee and K.J. Webb, "A temperature dependent non-linear analytical model for AlGaIn/GaN HEMT on SiC", *IEEE Trans. Microw. Theory Tech.* vol. 52, no. 1, pp. 2-9, Jan. 2004.